

## CHAPTER 4 DYNAMIC BEHAVIOR OF KBMFs

### 4.1 General

The chapter presents the analytical study to evaluate the behavior of the proposed system under seismic forces. The results including overall inelastic behavior and the response of important members were obtained from the nonlinear static and dynamic analyses using the modeling approach described in the past Chapters. Three-story conventional KBMFs with PR connections using two different types of braces are presented in this chapter.

### 4.2 Study Building

An example structure was used to study the seismic response of the proposed system. The plan view of the study building is shown in Figure 4.1. The lateral stiffness in the N-S direction of the frame is provided by two KBMFs while the lateral load resisting system in the E-W direction is assumed to be provided by conventional braced frame. In the N-S direction, each of the lateral load resisting frames is assumed to carry half of the total mass. The frame is assumed to be fixed at the ground level. The loading definition and floor masses of the three-story building are presented in Tables 4.1 and 4.2, respectively.

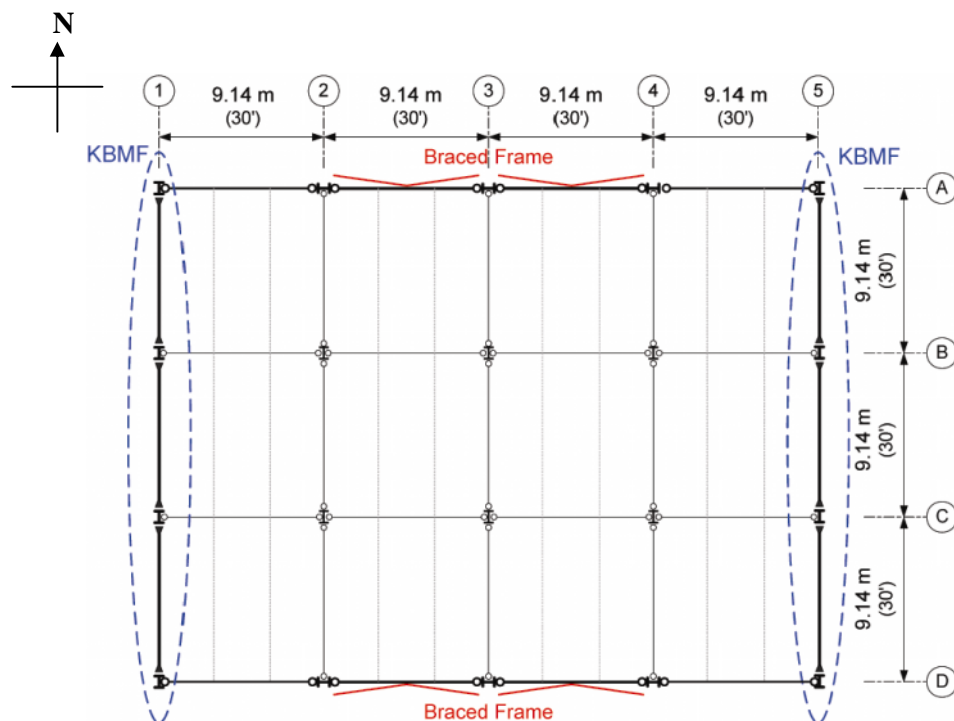


Figure 4.1 Plan View of Study Building [21].

**Table 4.1** Load Definition of Study Building [21].

Load Type	Definition	Load
Dead Load	For typical floor (for weight calculations), (kN/m <sup>2</sup> )	4.60
	For typical floor (for mass calculations), (kN/m <sup>2</sup> )	4.12
	For roof floor, (kN/m)	3.98
	Parapet on Roof (kN/m)	1.27
Dead Load due to Exterior Wall (full structure)	Typical floor (kN)	618.50
	Roof floor (kN)	312.48
Live Load	Typical floor, (kN/m <sup>2</sup> )	2.40
	Roof floor, (kN/m <sup>2</sup> )	2.40

**Table 4.2** Floor Masses of The Study Building [21].

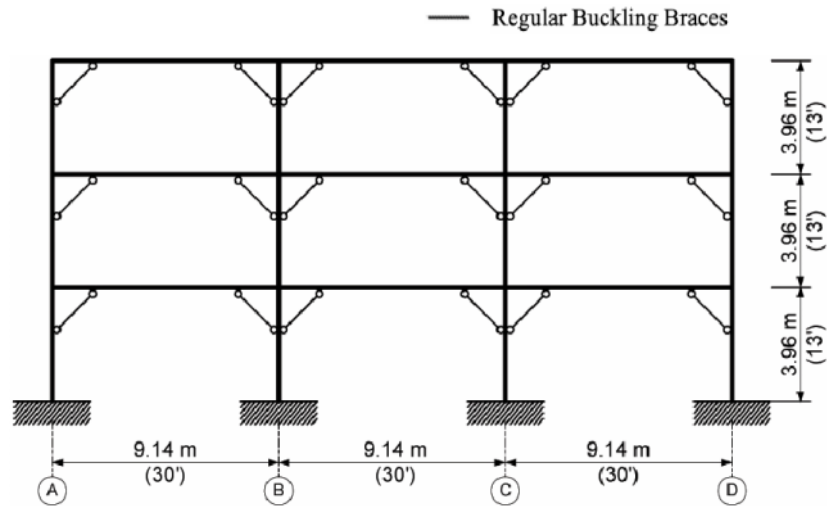
Floor No.	Floor Mass (kN.m/sec <sup>2</sup> )	Weight (kN)
Roof	533	5228
3	562	5517
2	562	5517

The design of the study building has been carried out by Srechai [21]. The design lateral forces were based on the performance-based plastic design (PBD) method. The procedures developed by Goel et al. [18] are applied to design the KBMF system. The equation of the design base shear coefficient and the lateral force distribution were described by Lee and Goel [18] and Srechai [21].

The three-story KBMF was designed using a target drift of 2.0 percent at the design basis earthquake level with the assumed yield drift at 1.0 percent. The estimated period,  $T$  of the frame was 0.75 second. The design base shear coefficient ( $V/W$ ) calculated by the procedures described above was 0.314. The design lateral forces at each floor level are shown in Table 4.3 and the resulting frame is shown in Figure 4.2.

**Table 4.3** Lateral Forces of KBMF based on PBD Procedure.

Floor	Height (in)	Lateral force (kN)
Roof	11.88	1442
3	7.92	758.7
2	3.96	353.8
G	0	0



Sectional properties of KBMF based on PBPD\*

Story	Exterior column	Interior column	Beam	Knee brace
1	W14 × 132	W14 × 176	W27 × 84	TS6 × 6 × 1/2
2	W14 × 132	W14 × 176	W24 × 84	TS5 × 5 × 1/2
3	W14 × 132	W14 × 176	W24 × 55	TS4 × 4 × 3/8

\*Section refers to ASTM standard.

**Figure 4.2** Three-Story of KBMF Study Frame [21].

### 4.3 KBMF with PR connections

In this study, welded beam-to-column connections in KBMF system were replaced by partially restrained (PR) connections. Bolted top and seat angle connection with double web angles typical were used to design the beam-to-column connections. Three-parameter power model considering nonlinear behaviors developed by Kishi and Chen [6,7] were employed to design PR connections in the three-story of KBMF frame. This model simulates the  $M-\theta$  behaviors using the mathematical expressions that consider material and geometric properties. The ultimate moment capacity of each connection was designed to be equal to the plastic moment of the connecting beam. Detailed design procedure is given in Appendix A. The member sizes of the KBMF with PR connections are shown in Table 4.4 and Figure 4.3.

**Table 4.4** Sectional Properties of PR Connection.

Connection Properties		Floor		
		2	3	Roof
Ultimate moment capacity (kN-m)		1060	945	600
Top and Bottom Angle	Angle*	L8×8×7/8	L8×8×7/8	L8×8×5/8
	Bolt diam (Column leg)	2-1 <sup>3</sup> / <sub>8</sub>	2-1 <sup>3</sup> / <sub>8</sub>	2-1 <sup>1</sup> / <sub>8</sub>
	Bolt diam (Beam leg)	4-1 <sup>3</sup> / <sub>8</sub>	4-1 <sup>3</sup> / <sub>8</sub>	4-1 <sup>1</sup> / <sub>8</sub>
Web Angle	Angle*	L6×6×3/4	L6×6×3/4	L6×6×1 <sup>4</sup> / <sub>25</sub>
	Bolt diam (Column leg)	5-1 <sup>1</sup> / <sub>8</sub>	5-1	5-1
	Bolt diam (Beam leg)	5-1 <sup>1</sup> / <sub>8</sub>	5-1	5-1

\*Section refers to ASTM standard.

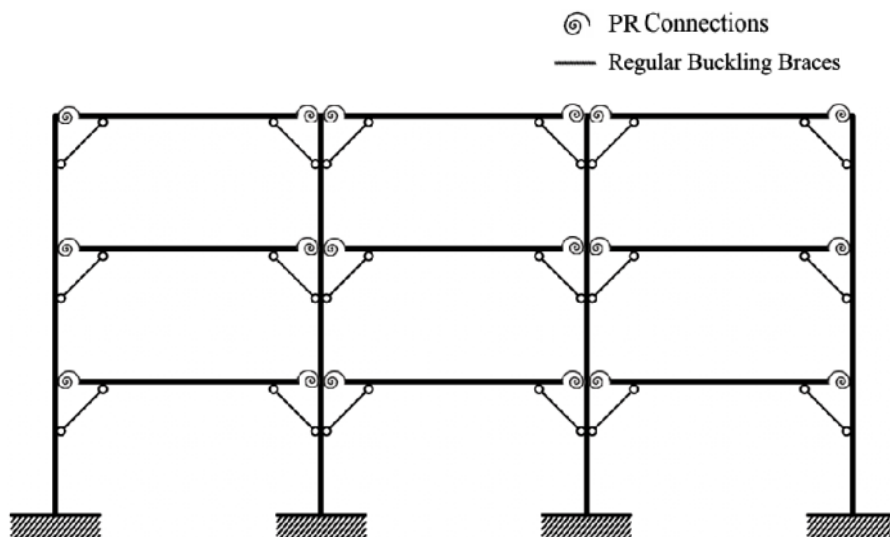
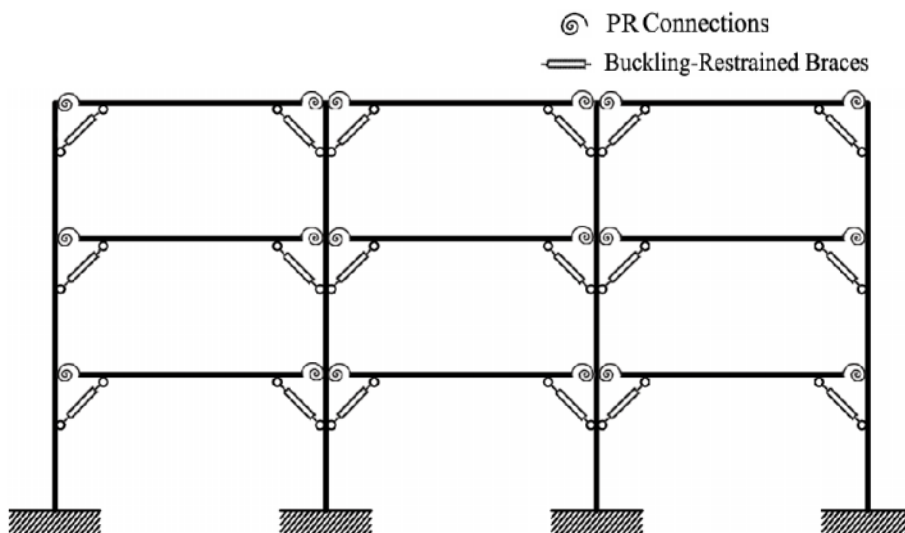


**Figure 4.3** KBMF with PR Connections Study Frame Used in Seismic Evaluation.

For the three-story KBMF with BRBs, the regular buckling braces in the frame at mentioned previously were replaced by BRBs. The yield strength of the braces was kept constant for both the buckling braces and BRBs. The behaviors of the BRBs were defined following the assumption indicated in section 3.2.6. The member sizes of KBMF with PR connections and BRBs are shown in Figure 4.4.



Sectional properties of BRB

Story	Core area (mm <sup>2</sup> )	Yield strength (kN)	BRB length (m)
1	6710	2310	2.6
2	4290	1480	2.6
3	3280	1130	2.6

**Figure 4.4** Three-Story KBMF with BRBs.

## 4.4 Methods of Analysis

Nonlinear static (pushover) and nonlinear dynamic analysis were employed to evaluate the KBMF with PR connections. A nonlinear analytical program called PERFORM-3D [17] was used.

### 4.4.1 Nonlinear Static (Pushover) Analysis

Nonlinear static analyses were carried out under the gravity and lateral loads. The gravity included the dead loads and 25 percent of live loads. PBPD design lateral force was used for increasing lateral forces. The analyses were performed up to the roof drift of 5 percent.

### 4.4.2 Nonlinear Dynamic Analysis

In the nonlinear dynamic analyses, the study frames were subjected to seven selected earthquake records scaled to represent the Design Basis Earthquake (DBE) and the Maximum Considered Earthquake (MCE) as specified by ASCE 7-10 [19]. The seven ground motions are referred to as LA02, LA06, LA08, LA10, LA14, LA16, and LA18. In this study, the scaling procedure for the DBE was based on the ASCE 7-10 [19] ground motion requirements for nonlinear dynamic analysis procedure. The selected ground motions are scaled such that their average spectra values between the periods of  $0.2T$  to  $1.5T$  are not less than those obtained from the design spectrum. The MCE ground motions are obtained by multiplying the DBE ground motions by a factor of 1.5. The scaled response spectra of the records (with 5% damping) and the one corresponding to the ASCE 7-10 [19] design acceleration spectra are shown in Figures 4.5 and 4.6 for the DBE and MCE levels. Table 4.5 summarizes the characteristics and the scaling factors of the seven records.

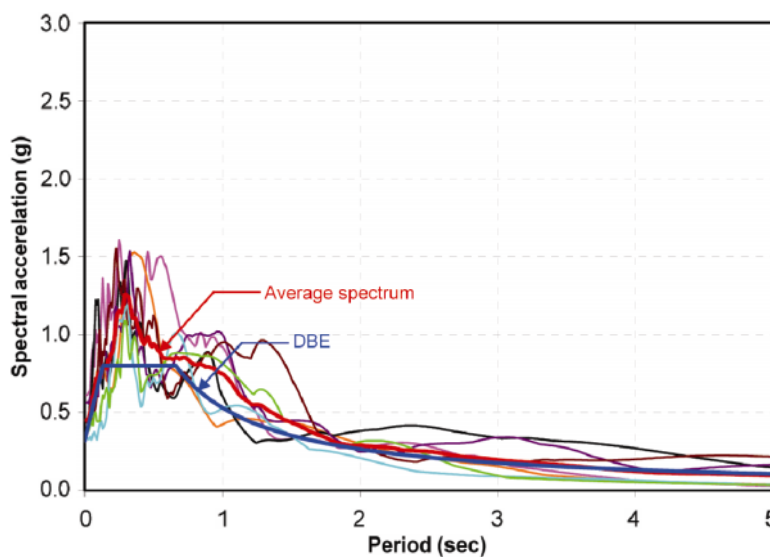


**Figure 4.5** Scaled Pseudo-Acceleration Spectra of DBE Ground Motions (5% Damping) [21].

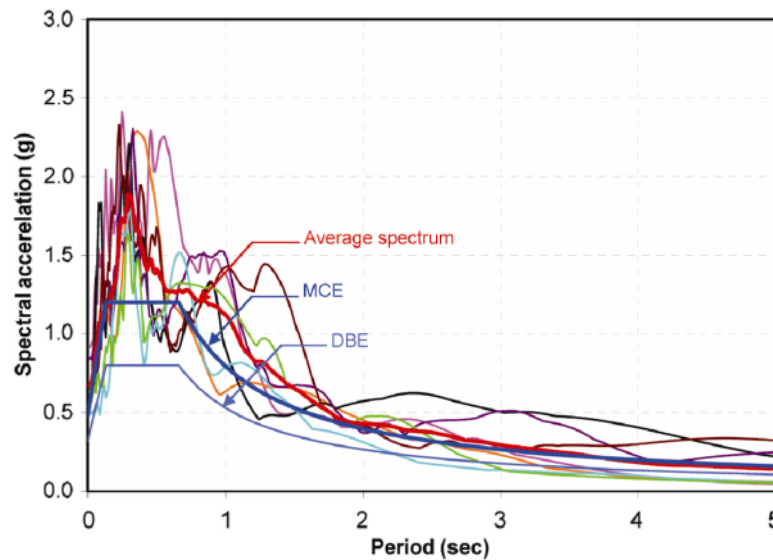


**Figure 4.6** Scaled Pseudo-Acceleration Spectra of MCE Ground Motions (5% Damping) [21].

**Table 4.5** Characteristics of Seven Selected Earthquake Records [21].

Identifier	Earthquake	DBE Scaled Peak Acc. (g)	MCE Scaled Peak Acc. (g)
LA02	Imperial Valley, 1940, El Centro	0.608	0.912
LA06	Imperial Valley, 1979, Array #06	0.376	0.564
LA08	Landers, 1992, Barstow	0.554	0.831
LA10	Landers, 1992, Yermo	0.432	0.648
LA14	Northridge, 1994, Newhall	0.329	0.494
LA16	Northridge, 1994, Rinaldi RS	0.364	0.546
LA18	Northridge, 1994, Sylmar	0.449	0.674

#### 4.5 Analytical Model of Study Building

The frame was modeled as three-story frame with fixed supports at the ground level using the same modeling techniques for the PR connections as described in Chapter 3. The floor masses were lumped and distributed at the beam-to-column connection nodes of the floor. Rayleigh Damping was employed to define the damping ratio which considers mass-proportional damping and stiffness-proportional damping. As follow:

$$[C] = a_0[M] \quad \text{and} \quad \zeta = \frac{a_0}{2} \frac{1}{\omega_n} \quad (4.1)$$

where  $[C]$ ,  $[M]$ , and  $[K]$  are the viscous damping, mass matrices and stiffness matrices of the system, respectively.  $a_0$  and  $a_1$  are the mass-proportional damping coefficient ( $\text{sec}^{-1}$ ) and the stiffness-proportional damping coefficient (sec).

The damping ratio for the  $n^{\text{th}}$  mode of the system is

$$\zeta_n = \frac{a_0}{2\omega_n} + \frac{a_1}{2}\omega_n \quad (4.2)$$

For applying this procedure to the model, the damping ratios of the first and second mode were defined as 2%. The damping ratios for modes higher than the second can be computed by Equation 4.2.

The effect of gravity loads was modeled by using distributed load in every span and concentrated force at each column. The gravity loads were found to be relatively small. For the lateral loads, it was distributed at every joints of each floor. P-delta was not included in the analysis. The analytical model of the study frame is shown in Figure 4.7.

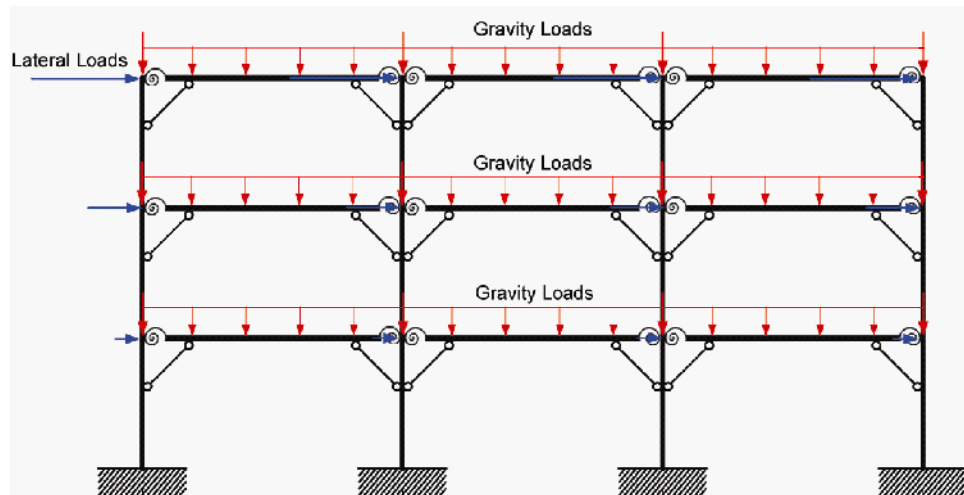


**Figure 4.7** Analytical Models of Three-Story KBMF.

## 4.6 Nonlinear Static Analysis of KBMF with PR connections

This section presents the results from analytical studies of the KBMF with PR connections. Two types of knee braces are considered in this analysis: regular buckling braces and buckling restrained braces (BRBs). The results including overall inelastic behavior and response of key members were obtained from nonlinear static analyses. The main findings from the study of this frame are as follows:

### 4.6.1 Pushover Curves

The plots of the base shear coefficient versus roof drift of the KBMF frames are shown in Figure 4.8. The results of KBMF with welded connections from Srechai [21] are also presented for comparison. As can be seen, KBMFs with PR connections have relatively the same strength and initial stiffness as the KBMF with welded connection. The response of the KBMF with welded connection was elastic up to a drift level of approximately 0.85% while the response of the KBMFs with PR connections was elastic up to 1% drift. The comparison indicates that the flexibility of PR connections affects the yielding of the KBMF system.

After 1% drift, the inelastic activity then quickly spread out, resulting in a significant reduction in the lateral stiffness. The figure shows that the post-yielding stiffness of the frame with PR connections and buckling braces is less than that of the other frames by approximately 10 percents. The post-yielding stiffness of other two frames is similar. The results show that the KBMF with PR connections is comparable to the KBMF with rigid connections in terms of strength and stiffness.

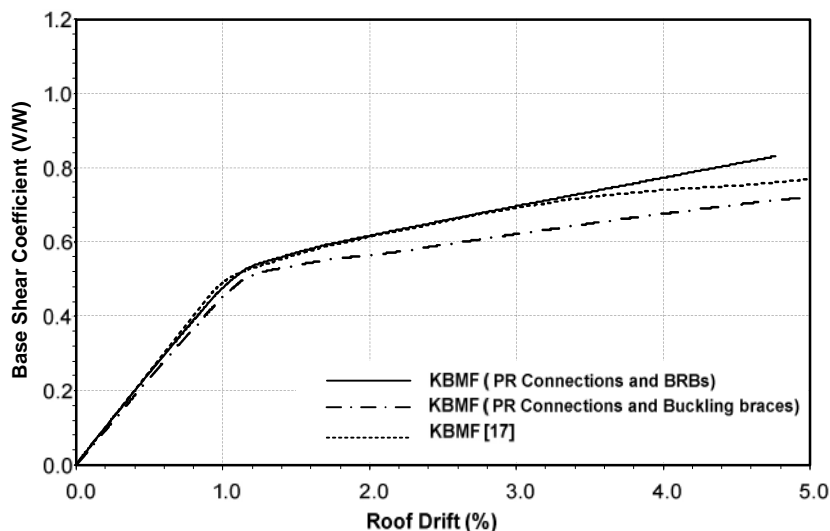


**Figure 4.8** Pushover Curve of KBMFs.

The plots of the base shear versus roof drift of the two KBMFs with PR connections are shown in Figure 4.9. The figure demonstrates the sequence of inelastic activities under increasing lateral forces. Key information of the response is presented in Table 4.6. As can be seen, the response of the frames was elastic up to a drift level of 1.10%, when the first set of plastic hinge formed. The results indicate that the two frames have the similar strength and stiffness in the elastic stage. After yielding, the behavior of the two frames directly depends on the strength of the knee braces

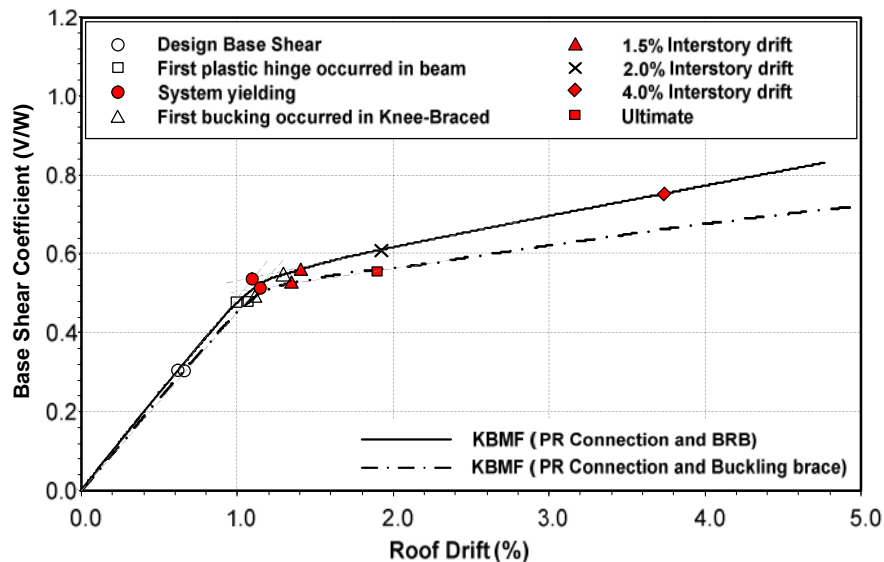
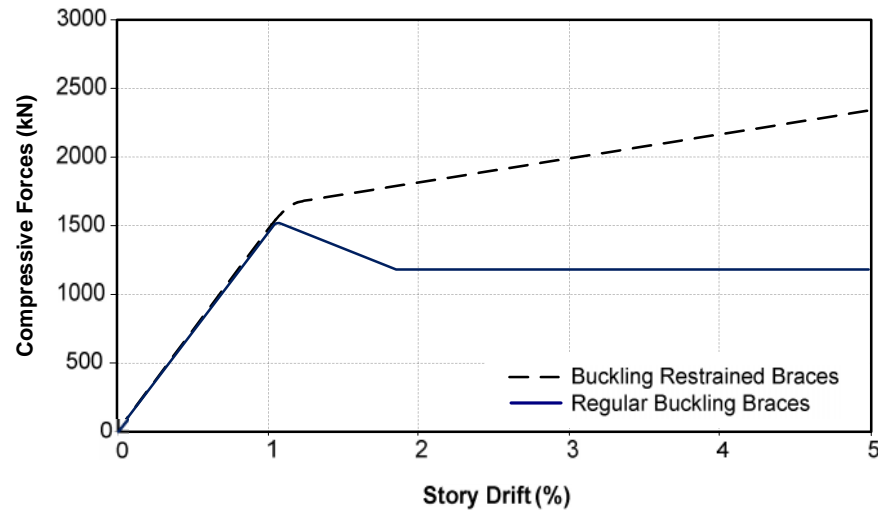


**Figure 4.9** Base Shear Versus Roof Drift From Nonlinear Static Analysis of KBMF with PR Connections.

**Table 4.6** Results From Nonlinear Static Analysis of Three-Story Structures.

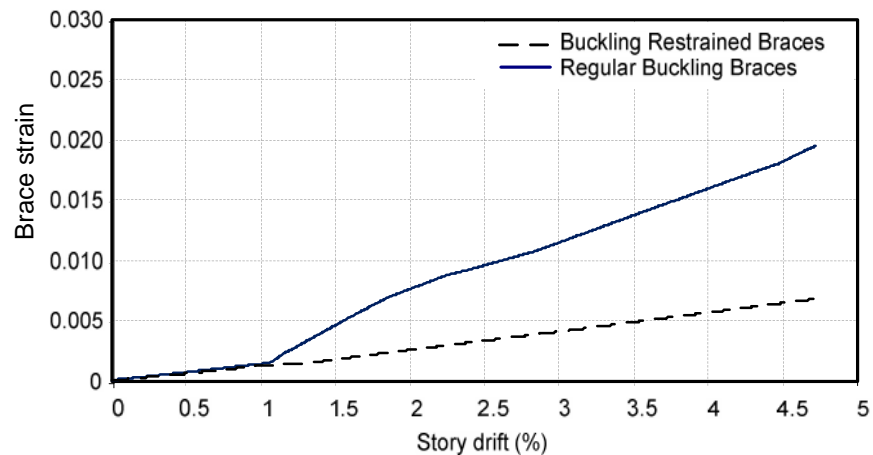
Characteristic of structure	Structures Model	
	KBMF with PR Con.	KBMF with PR Con. and BRB
Period, $T$ (sec)	0.79	0.78
Base shear at system yielding, $V_y/W$	0.46	0.48
Roof drift at system yielding, $\Delta_y$	1.12	1.08
Roof drift at inter-story drift 1.5 % , $\Delta_{1.5\%}$	1.35	1.37
Roof drift at inter-story drift 2.0 % , $\Delta_{2.0\%}$	-	1.83
Roof drift at inter-story drift 4.0 % , $\Delta_{4.0\%}$	-	3.76

Figure 4.10 shows the compressive forces in the knee braces. After the first plastic hinge occurred in the beam, the inelastic activity spread out into the knee braces. For the frame with conventional braces, the first buckling occurred in the brace immediately after plastic hinge formed. The braces buckled in compression and experienced strength loss resulting in the overall strength loss and large reduction in lateral stiffness of the frame. On the other hand, BRBs in the frame could carry the axial load without buckling. The braces yielded in tension and compression with strain hardening resulting in a stable response.



**Figure 4.10** Compressive Internal Forces of Two Different Types of Braces.

Figure 4.11 shows the strain values in the braces at different drift levels. As can be seen, the strain of the BRB is less than that of the regular buckling brace at the same drift level. The buckling of the regular buckling braces reduces the stiffness of the braces in resulting easily to deform when compared to that which the BRBs. It can be deduced that the regular brace would eventually fracture under a smaller drift value when compared to that causes a fracture in the BRBs.



**Figure 4.11** Strain in Knee Braces.

Figures 4.12 and 4.13 show the inter-story drift profiles upto ultimate limit stage of the KBMFs with regular buckling braces and BRBs, respectively. The ultimate inter-story drift of the frames was defined by the fracture in the knee braces or the BRBs. The value of the ductility limit of the braces was obtained by considering the test results under cyclic loading. For regular buckling braces, the first fracture of the stocky braces occurs approximately at a ductility of 4 [22]. For BRBs, the average value of the deformation limit was obtained from collected test results which were summarized by Steel Tips [23]. An axial strain of 2.23% was [23] used to indicate the failure in the BRBs.

The pushover plot shows that the frame with buckling braces could only deform upto 2.0% inter-story drift level when the first fracture was detected in the buckling braces. The results show that this frame reached the ultimate limit stage at a very small inter-story drift. On the other hand, BRB could resist the lateral with deformation larger than 4.0% inter-story drift level out with fracture. The results indicate that buckling braces are not suitable for KBMF with PR connections.

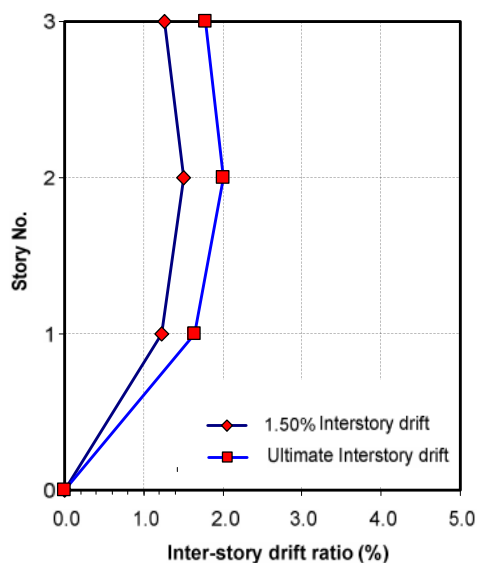


**Figure 4.12** Inter-Story Drift Profiles of KBMF with Buckling Braces.

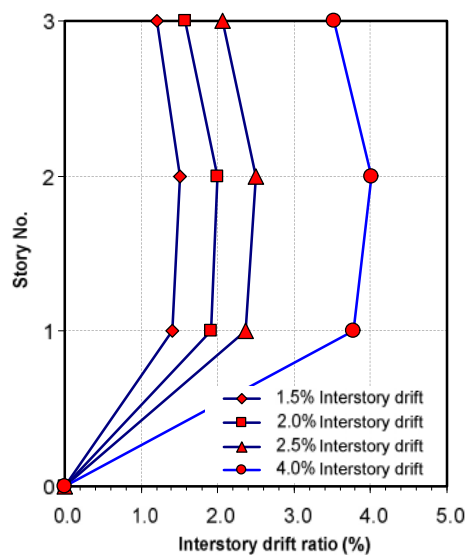


**Figure 4.13** Inter-Story Drift Profiles of KBMF with BRBs.

## 4.7 Nonlinear Dynamic Analysis of KBMF with PR connections

A series of nonlinear dynamic analyses was carried out to investigate the seismic behavior of the KBMF with PR connections. Two different types of knee braces in KBMFs, regular-buckling braces and BRBs, were considered. The DBE and MCE ground motions were employed to evaluate these structures. Under the DBE ground motions, the story drifts must be less than the limit of 2.5% as stipulated in ASCE 7-10 [19], and under the MCE ground motions, the frame is allowed to suffer significant damage but should not reach its ultimate state.

### 4.7.1 Dynamic Response under DBE Ground Motions

The envelopes of maximum inter-story drifts under DBE ground motions of the KBMFs using two different types of braces are shown in Figures 4.14 and 4.15. As can be seen, the maximum inter-story drifts of both frames under this level were much closer to the target drift (2.0%) and less than 2.5% as provided by ASCE 7-10 [19]. The median and mean-plus-one-standard-deviation values show that the maximum inter-story drifts of both frames occurred in the first story. The maximum inter-story drifts of both frames occurred under the LA16 ground motion.

Figures 4.16 and 4.17 show the maximum average and maximum mean-plus-one-standard-deviation values of inter-story drifts of the two frames. The maximum average inter-story drifts of both frames were approximately 1.5%. For the maximum mean-plus-one-standard-deviation values, the drift of the frame with conventional braces is very close to the ultimate drift limit in the first story (1.65% inter-story drift corresponding to the first fracture of a knee brace). On the other hand, the maximum value of mean-plus-one-standard-deviation inter-story drift of the frame with BRBs was 1.9%.

Figures 4.18 and 4.19 show the inelastic activities of the frames with regular and BRB braces under the LA10 of DBE ground motions. Figures 4.20 and 4.21 show the inelastic activities of both frames under the LA16 of DBE ground motions. The selected ground motions, LA10 and LA16, closely represent the median and the maximum response of all selected ground motions. The results indicate that the plastic hinges occurred at the ends of beam outside knee regions and the column bases, and the buckling and yielding occurred in some of the knee braces. As can be seen, buckling and yielding were detected in all the regular buckling braces on the second and the third stories under LA10 and were detected at the right hand side of each bay in all floors under LA16. On the other hand, yielding of BRB was detected in the KBMF with BRBs on the second story only.

The comparison indicates that the frame with buckling braces would suffer damage from DBE ground motions when compare to the frame with BRBs. Many regular buckling braces in this frame should be repaired after an earthquake resulting in a larger repair cost. Nevertheless, the results show that KBMF with PR connections did not reach the ultimate limit stage under DBE ground motion. For the KBMF with BRBs, the results show that this frame performed well under DBE ground motions.

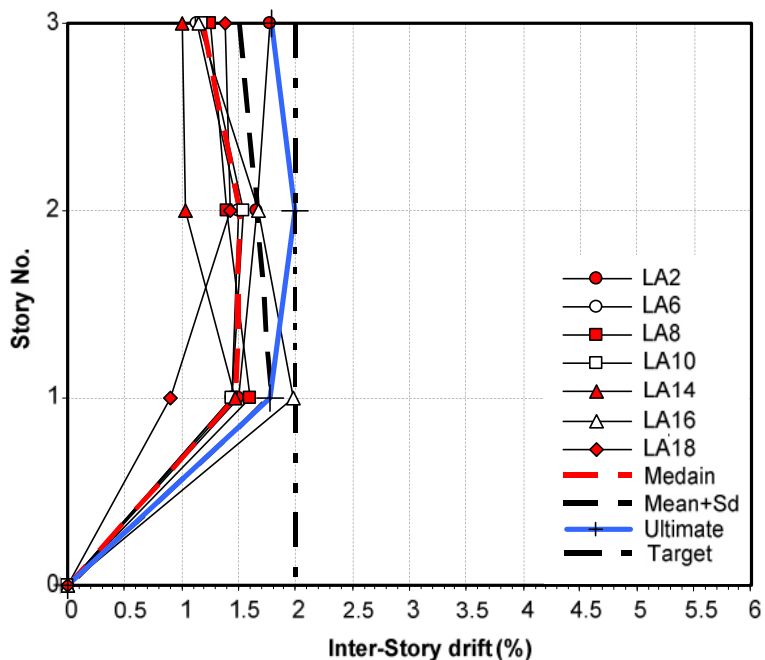


**Figure 4.14** Maximum Inter-Story Drift Profiles of KBMF Regular Buckling Braces under DBE Ground Motions.

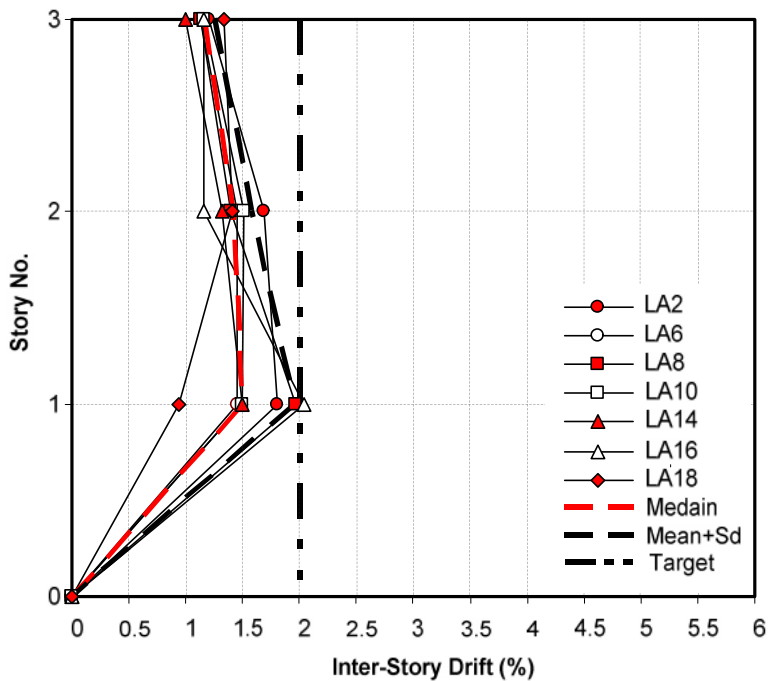


**Figure 4.15** Maximum Inter-Story Drift Profiles of KBMF with BRBs under DBE Ground Motions.

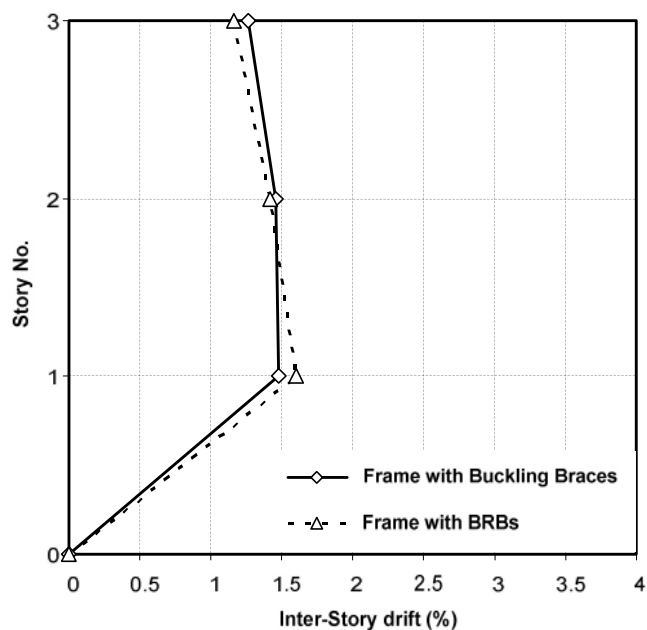


**Figure 4.16** Maximum Average Inter-Story Drifts of Three-Story Study Frames under DBE Ground Motions.

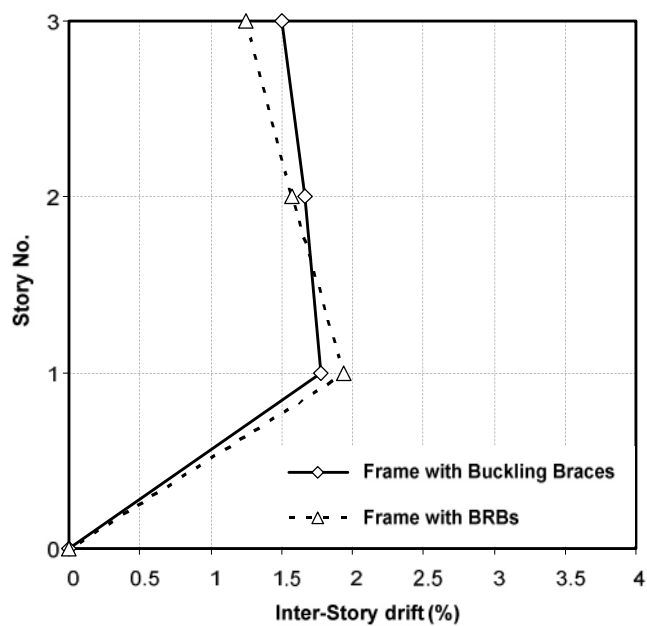


**Figure 4.17** Maximum Mean-Plus-One-Standard-Deviation Values Inter-Story Drift of Three-Story Study Frames under DBE Ground Motions.

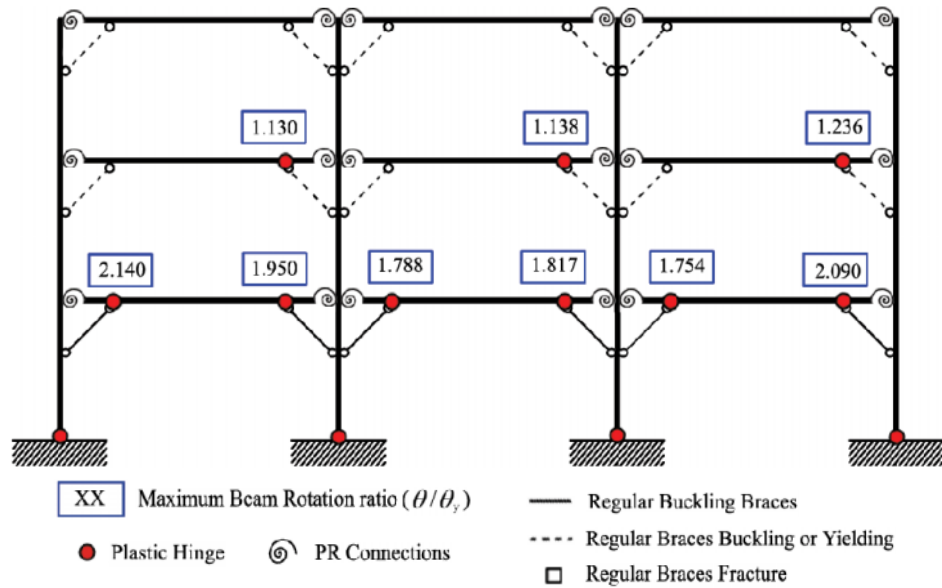


**Figure 4.18** Inelastic Activities of KBMF with Conventional Braces under Selected DBE Ground Motion (LA10).

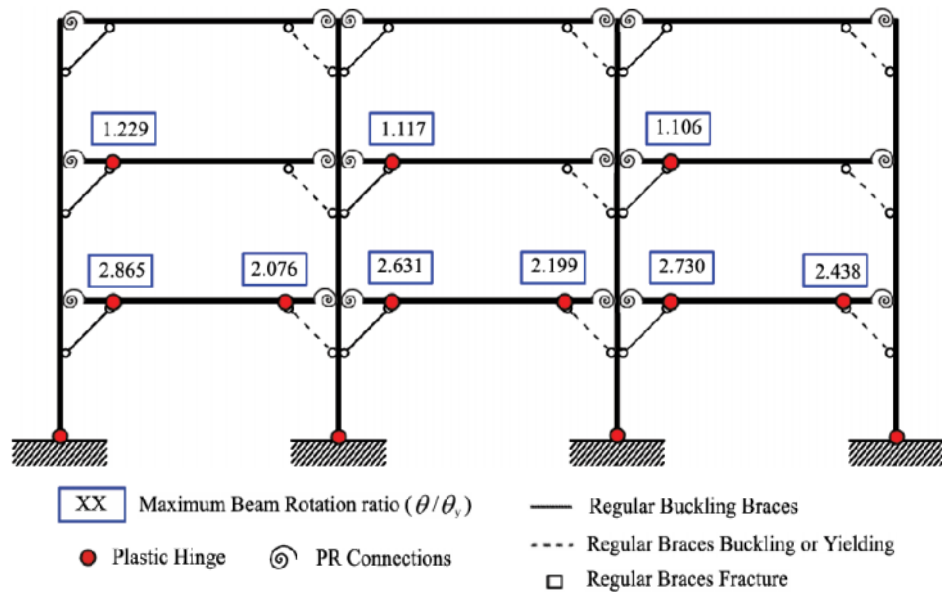


**Figure 4.19** Inelastic Activities of KBMF with BRBs under Selected DBE Ground Motion (LA10).

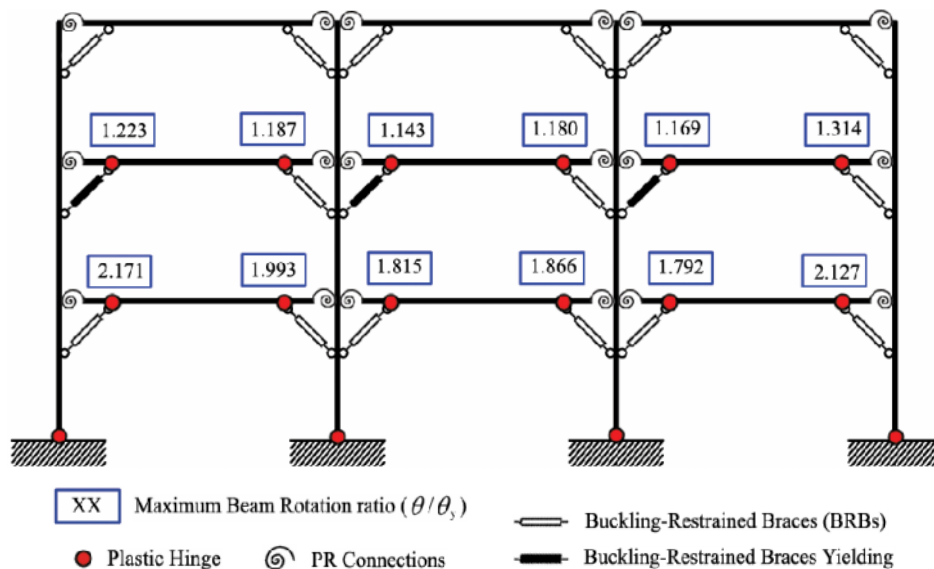


**Figure 4.20** Inelastic Activities of KBMF with Conventional Braces under Selected DBE Ground Motion (LA16).

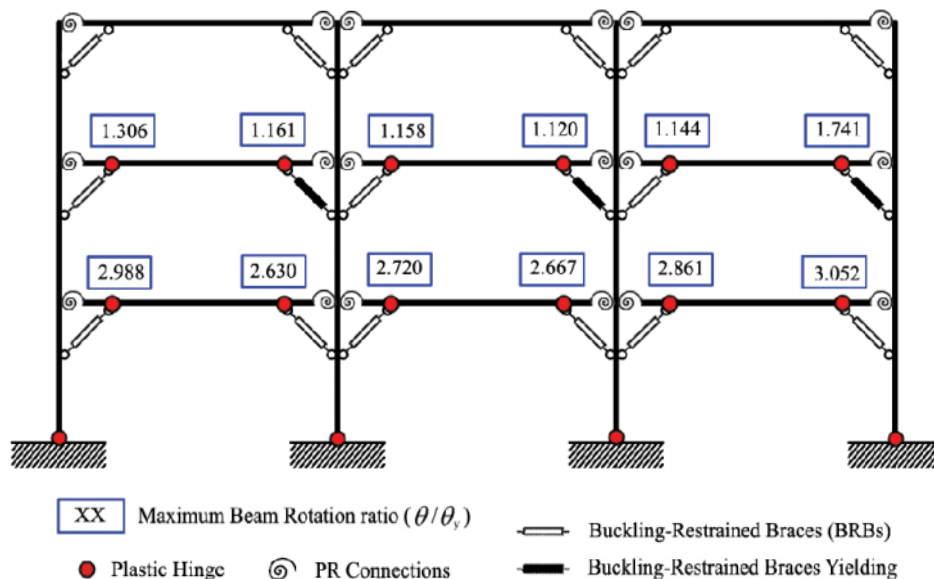


**Figure 4.21** Inelastic Activities of KBMF with BRBs under Selected DBE Ground Motion (LA16).

The response of the connections is examined in Figure 4.22. The figure shows the maximum normalized moment with respect to the ultimate moment ( $M_u$ ) under DBE ground motions of the two frames. It can be seen that the values of both frames did not reach the value of 1, meaning that the connection did not reach the ultimate limit state. The results show that the values of both frames under the LA10 ground motion are similar. The values of the frame with buckling braces are more than those of the frame with BRBs under the LA16 ground motion. The maximum value of 0.68 was found at joint number 2 under LA16. Both figures indicate that the PR connections were capable of resisting the DBE ground motions.

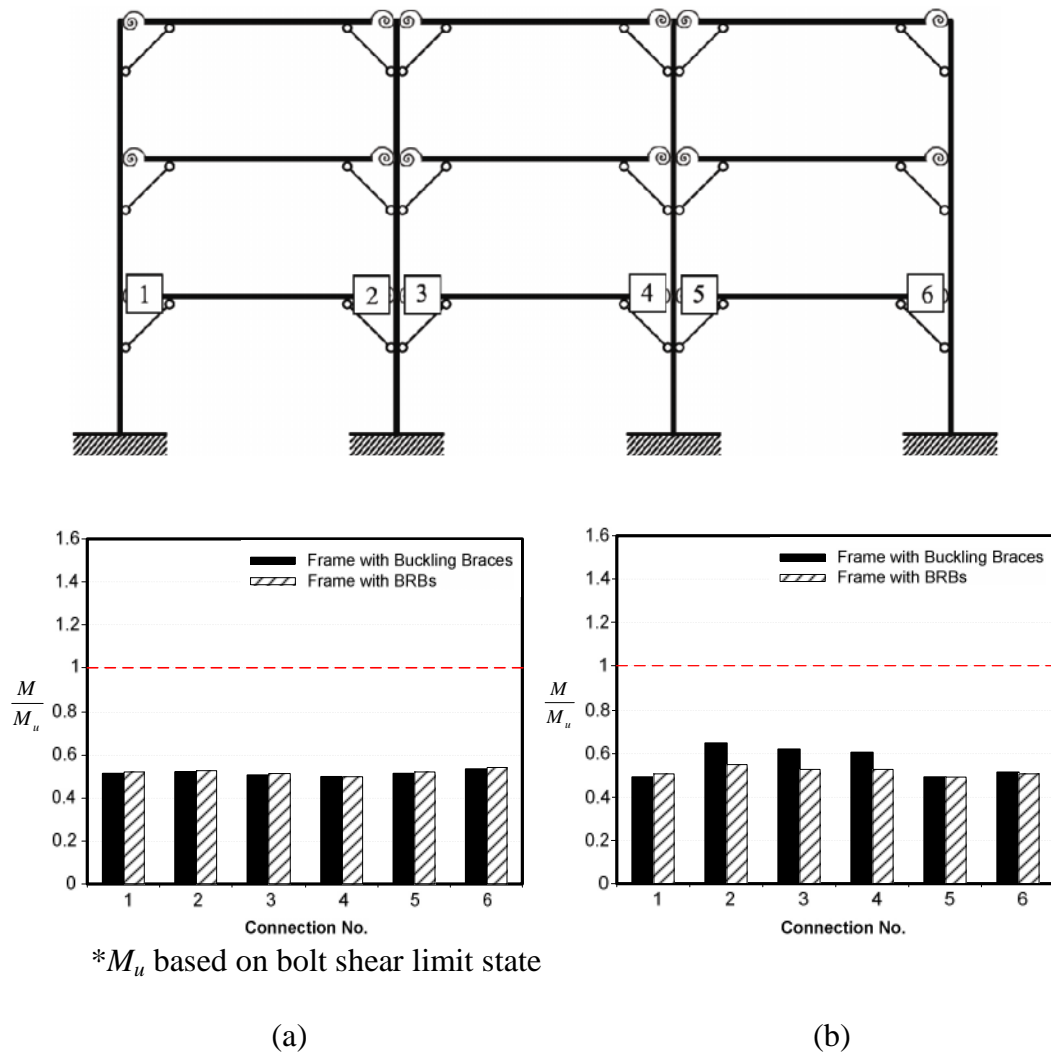


**Figure 4.22** Normalized Moment at Connections under DBE Ground Motions (a) LA10, (b) LA16.

### 4.7.2 Dynamic Response under MCE ground Motions

Under the MCE ground motions, the values of the inter-story drift increase by approximately 1.5 times. For this level, the frames are allowed to suffer significant damage but should not reach its ultimate state. Figures 4.23 and 4.24 show the envelope of the maximum inter-story drift under MCE ground motions. Based on the figures, the median and mean-plus-one-standard-deviation values show that the maximum inter-story drifts occurred in the first story of each frame. The maximum inter-story of both frames occurred under the LA16 ground motion. The values are approximately 3.8% and 3.5% drifts for the frame with regular braces and the frame with BRBs, respectively.

Figures 4.25 and 4.26 show the maximum average drift and maximum mean-plus-one-standard-deviation drift values of the two frames. As can be seen, the maximum values occurred in the first story. The maximum average inter-story drifts are approximately 2.5% for the two frames, and the mean-plus-one-standard-deviation values of the inter-story drifts are approximately 3.2% and 3.4% for the frame with conventional braces and the frame with BRBs, respectively. The results show that the inter-story drifts in the first story of both frames are similar, but are different in the second and the third stories. The inter-story drifts in the second and the third stories of the frame with BRBs are less than those of the frame with buckling braces, especially in the third story.

Figures 4.27 and 4.28 show the inelastic activities of the two frames under the LA10 ground motion. Figures 4.29 and 4.30 show the inelastic activities of the frames under the LA16 ground motion. The selected ground motions closely represent the median and maximum response under the MCE ground motion level. As can be seen, the plastic hinges occurred at the ends of beam outside knee regions and the column bases. Based on the figures, both frames suffered more damage under the MCE level than the DBE level. Under the LA10 ground motion, the buckling and yielding occurred in all of regular buckling braces. The inelastic activities of the frame with regular braces indicated that some of the braces fractured signifying the ultimate state under the LA16 ground motion. For the frame with BRBs, the yielding was detected but the fracture did not occur under this MCE level.

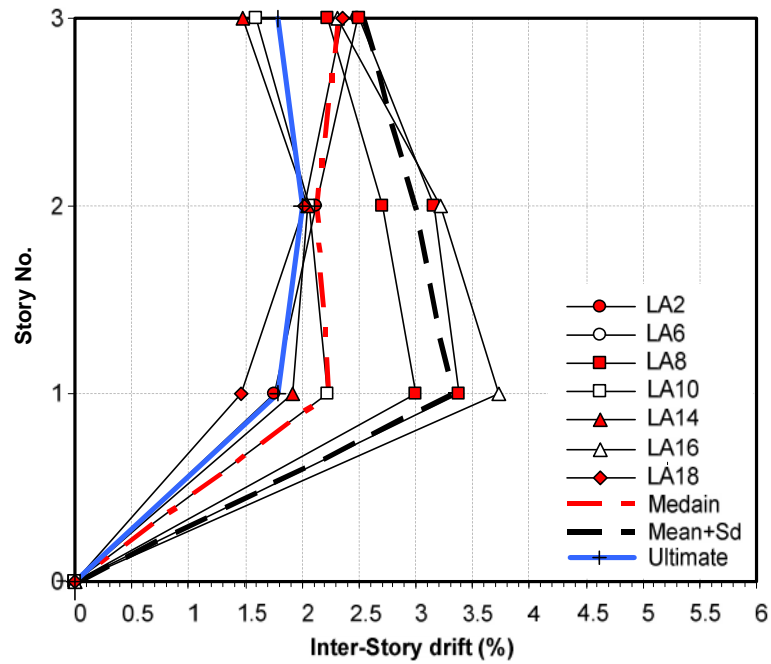


**Figure 4.23** Maximum Inter-Story Drift Profiles of KBMF with Regular Buckling Braces under MCE Ground Motions.

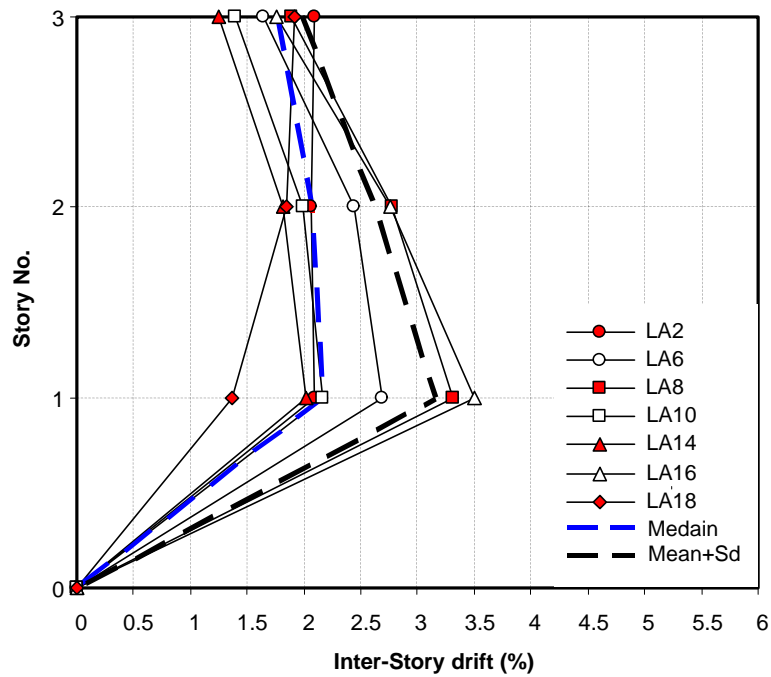


**Figure 4.24** Maximum Inter-Story Drift Profiles of KBMF with BRBs under MCE Ground Motions.

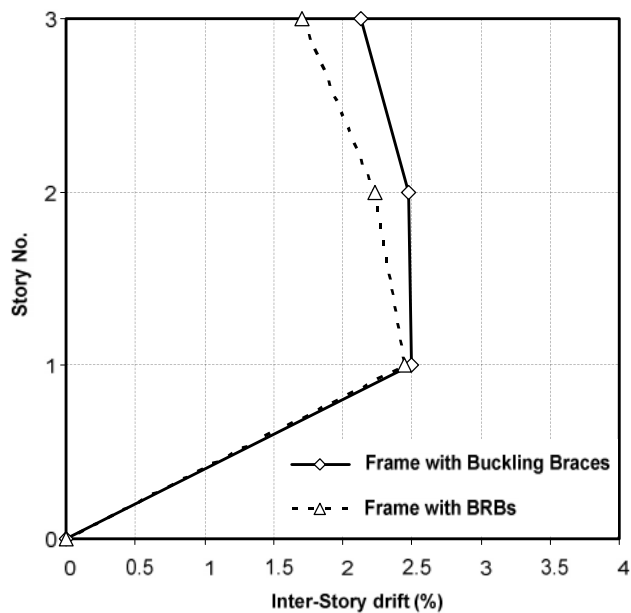


**Figure 4.25** Maximum Average Inter-Story Drifts under MCE Ground Motions.

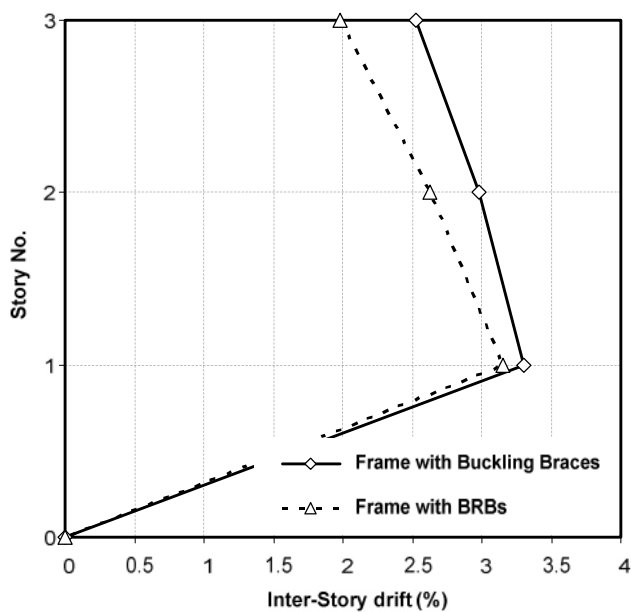


**Figure 4.26** Maximum Mean-Plus-One-Standard-Deviation Inter-Story Drifts under MCE Ground Motions.

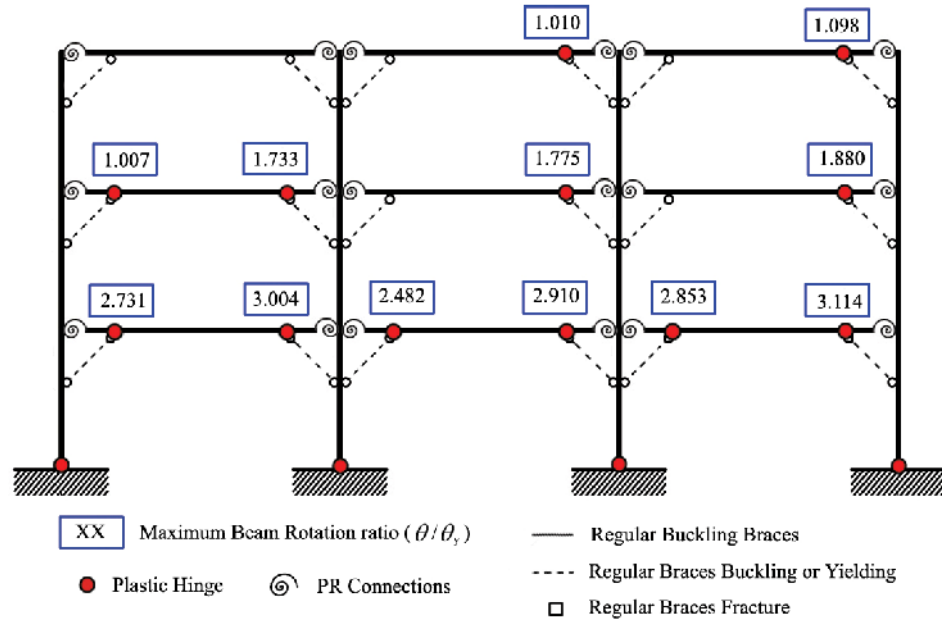


**Figure 4.27** Inelastic Activities of KBMF with Conventional Braces under Selected MCE Ground Motion (LA10).

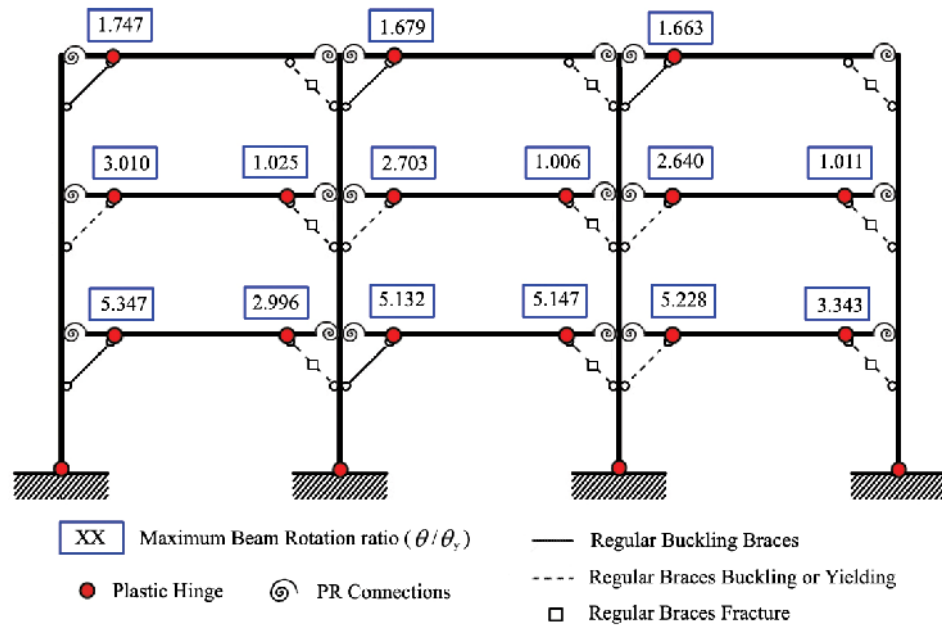


**Figure 4.28** Inelastic Activities of KBMF with BRBs under Selected MCE Ground Motion (LA10).

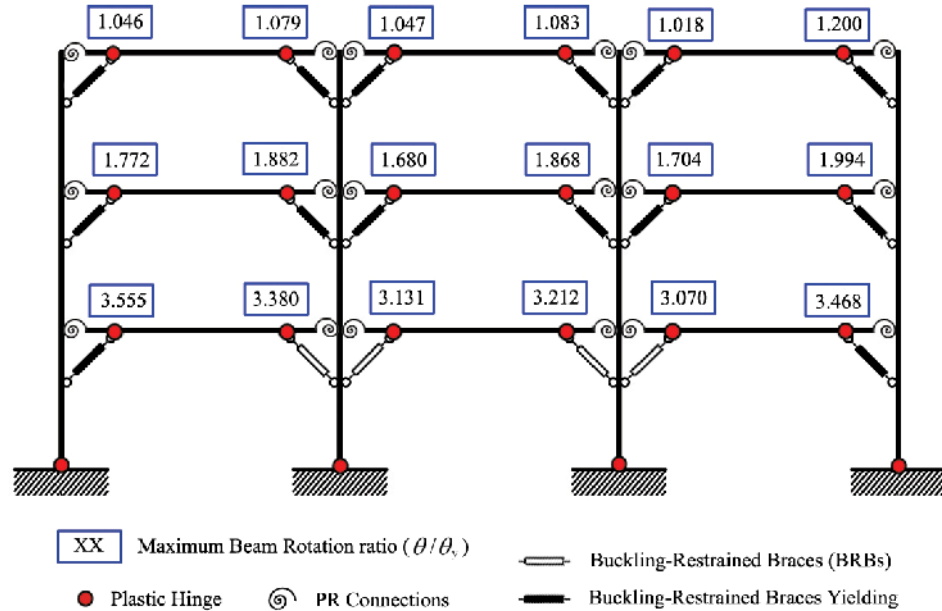


**Figure 4.29** Inelastic Activities of KBMF with Conventional Braces under Selected MCE Ground Motion (LA16).

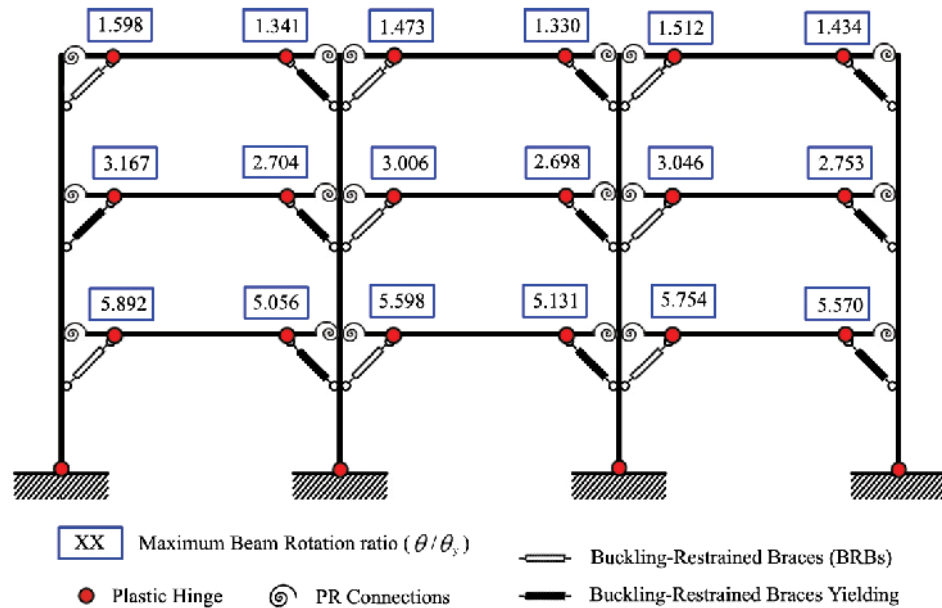


**Figure 4.30** Inelastic Activities of KBMF with BRBs under Selected MCE Ground Motion (LA16).

The response of the connections is examined in Figure 4.31. The figure shows the maximum normalized moment with respect to the ultimate moment ( $M_u$ ) under the MCE ground motions of the two frames. The results show that the connections suffered more damage under this level of ground motion. The maximum value of normalized moment under the LA10 ground motion was about 0.75. Under the LA16, the result clearly shows that three connections in the first story of the frame with regular braces reached the ultimate limit state. On the contrary, the connections of the frame with BRBs did not.

Based on the observed connection behavior, it can be seen that the frame with BRBs provided superior seismic performance than the frame with buckling braces. The presence of BRBs can reduce the PR connections deformation under seismic forces and the connections do not reach ultimate limit state.

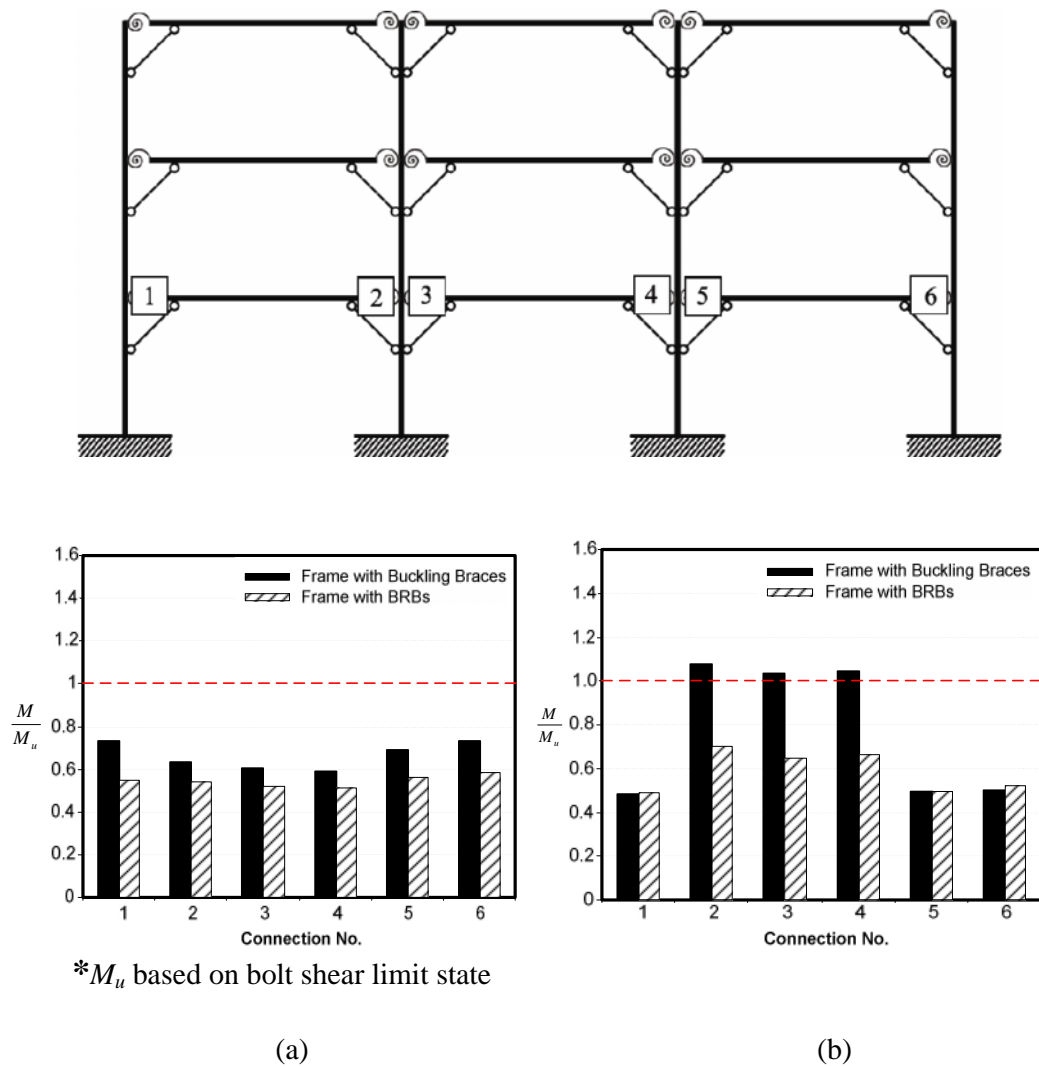


**Figure 4.31** Normalized Moment at Connections under MCE Ground Motions (a) LA10, (b) LA16.

Overall, it can be seen that PR connections can be used in KBMFs but not in combination with regular buckling braces because the flexibility of the connections in conjunction with the buckling of the regular braces may result in early fracture of the braces. It can be deduced that the regular brace would eventually fracture under a small drift value. Based on the observed behavior, BRBs can improve the dynamic behavior of the KBMF system. The elements can yield under tension and compression without buckling. The frame with BRBs can be used successfully to resist seismic forces under the both levels of ground motions.